

Notes

Boron–Nitrogen Coordination Polymers Bearing Ferrocene in the Main Chain

Manja Grosche,[†] Eberhardt Herdtweck,[†] Frank Peters,[†] and Matthias Wagner^{*,‡}

Anorganisch-chemisches Institut, Technische Universität München, Lichtenbergstrasse 4, D-85747 Garching b. München, Germany, and Institut für Anorganische Chemie, Johann Wolfgang Goethe-Universität Frankfurt, Marie-Curie-Strasse 11, D-60439 Frankfurt am Main, Germany

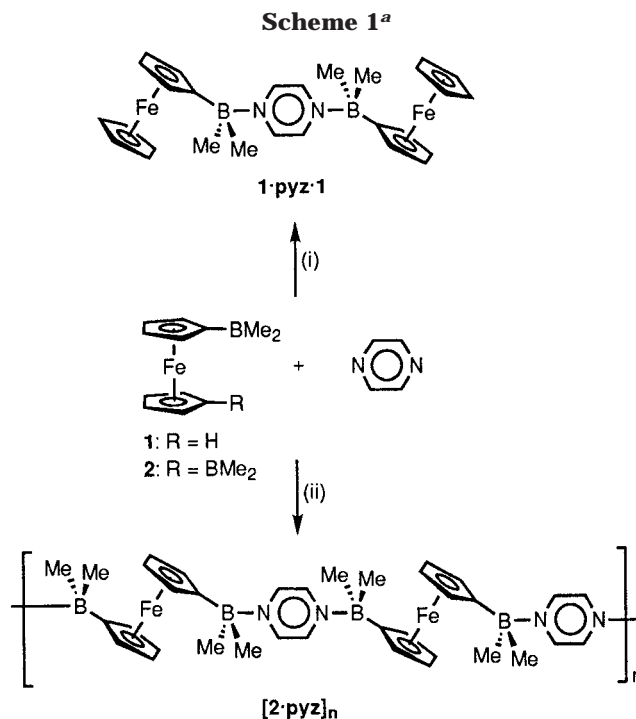
Received July 27, 1999

Summary: The reaction of 1,1'-fc(BMe₂)₂ (**2**) with pyrazine gives a novel poly(ferrocene) [2·pyz]_n, which has been structurally characterized by X-ray crystallography [fc = (C₅H₄)₂Fe; pyz = pyrazine]. The unusual dark green color of the solid material is indicative of charge-transfer interactions between the iron centers and the electron-poor pyrazine adduct bridges.

Introduction

Metal-containing macromolecules have been shown to possess interesting electrical, magnetical, and optical characteristics as a result of electron delocalization.¹ The favorable electrochemical properties of the ferrocene nucleus make this molecule a particularly promising candidate for the incorporation into polymer chains. Up to now, three major pathways to poly(ferrocenes) have been developed: (i) polycondensation reactions using difunctional ferrocenes (e.g., ferrocene-containing polyesters, polyamides, and polyureas),¹ (ii) the synthesis of ferrocene derivatives bearing polymerizable substituents (e.g., vinylferrocene),¹ (iii) the thermal^{2,3} or catalytic⁴ ring-opening polymerization of strained [1]- and [2]-ferrocenophanes.

Our group is interested in developing novel synthetic routes to these low-dimensional materials. Here we report on the synthesis and structural characterization of a dinuclear complex **1**·pyz·**1** and of a poly(ferrocene) [2·pyz]_n, in which the polymer backbone consists of diborylated units **2**,⁵ linked by pyrazine (pyz) bridges (Scheme 1). This approach is based on the facile formation of boron–nitrogen adduct bonds, thereby combining the advantages of coordination polymer synthesis with the unique properties of ferrocene building blocks.



^a (i) 2 **1** + 1 pyz, toluene; (ii) 2n **2** + 2n pyz, toluene.

Results and Discussion

We have already prepared a related poly(ferrocene) with 4,4'-bipyridine bridges and shown its molecular architecture to promote charge transfer along the polymeric rod.⁶ The macromolecular nature of this material was proven by an end group analysis based on infrared spectroscopy. However, despite numerous efforts, single crystals suitable for a structure determination by X-ray diffraction were not obtained. In the case of [2·pyz]_n, however, dark green, almost black, X-ray quality crystals could be grown at 5 °C by layering **2** in CH₂Cl₂ with a toluene solution of pyrazine. In a similar way we have prepared the dinuclear reference

* Corresponding author. Telefax: (internat.) +49(0)69/798-29188. E-mail: Matthias.Wagner@chemie.uni-frankfurt.de.

[†] Technische Universität München.

[‡] Johann Wolfgang Goethe-Universität Frankfurt.

(1) Manners, I. *Angew. Chem.* **1996**, *108*, 1712; *Angew. Chem., Int. Ed. Engl.* **1996**, *35*, 1602.

(2) Foucher, D. A.; Tang, B.-Z.; Manners, I. *J. Am. Chem. Soc.* **1992**, *114*, 6246.

(3) Manners, I. *Adv. Organomet. Chem.* **1995**, *37*, 131.

(4) Sheridan, J. B.; Temple, K.; Lough, A. J.; Manners, I. *J. Chem. Soc., Dalton Trans.* **1997**, 711.

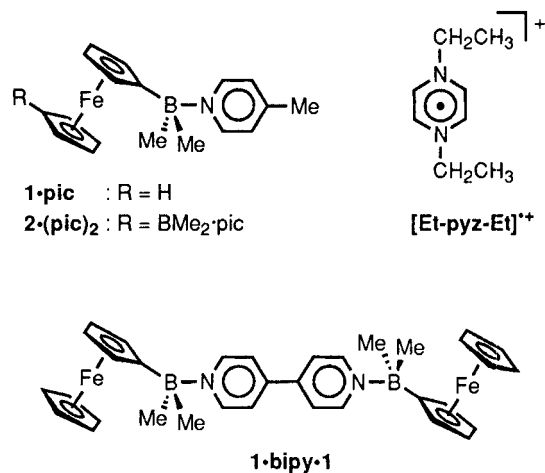
(5) Ruf, W.; Renk, T.; Siebert, W. *Z. Naturforsch. B* **1976**, *31b*, 1028.

(6) (a) Fontani, M.; Peters, F.; Scherer, W.; Wachter, W.; Wagner, M.; Zanello, P. *Eur. J. Inorg. Chem.* **1998**, 1453. (b) Fontani, M.; Peters, F.; Scherer, W.; Wachter, W.; Wagner, M.; Zanello, P. *Eur. J. Inorg. Chem.* **1998**, 2087.

Table 1. Crystal Data and Structure Refinement Details of **1-pyz·1** and **[2-pyz]_n**

	1-pyz·1	[2-pyz]_n·2C₇H₈
formula	C ₂₈ H ₃₄ B ₂ Fe ₂ N ₂	C ₃₂ H ₄₀ B ₂ FeN ₂
fw	531.91	530.15
cryst dimen, mm	0.94 × 0.15 × 0.15	0.50 × 0.30 × 0.13
cryst syst	monoclinic	monoclinic
space group	<i>P</i> 2 ₁ / <i>n</i> (No. 14)	<i>A</i> 2/ <i>n</i> (No. 15)
temp, °C	−110 ± 3	20 ± 1
<i>a</i> , Å	5.976(2)	8.0084(5)
<i>b</i> , Å	16.620(2)	16.7786(14)
<i>c</i> , Å	12.874(4)	21.9368(10)
β, deg	91.08(2)	100.298(6)
<i>V</i> , Å ³	1278.4(6)	2900.2(3)
<i>D_c</i> , g cm ^{−3}	1.382	1.214
<i>Z</i>	2	4
radiation	Mo Kα, 0.71073 Å	Mo Kα, 0.71073 Å
no. of total reflns	2846	9460
no. of uniq reflns	2507	1264
no. of obsd reflns	2220 [<i>I</i> > 2σ(<i>I</i>)]	1060 [<i>I</i> > 2σ(<i>I</i>)]
no. of params	222	168
μ, cm ^{−1}	11.5	5.4
final R1 ^a	0.0555 [all data]	0.0383 [all data]
final wR2 ^b	0.1290 [all data]	0.0731 [all data]
GOOF ^c	1.148	1.032

^a R1 = Σ(|*F_o*| − |*F_c*|)/Σ|*F_o*|. ^b wR2 = [Σw(*F_o*² − *F_c*²)²/Σw(*F_o*²)²]^{1/2}. ^c GOOF = [Σw(*F_o*² − *F_c*²)²/(NO − NV)]^{1/2}.

Scheme 2^a

^a Reference compounds **1-pic**, **2-(pic)₂**, **[Et-pyz-Et]⁺**, and **1-bipy·1**.

system **1-pyz·1**, which readily crystallizes from toluene/hexane (1:1) at −30 °C (red-brown needles). In the solid state, both **1-pyz·1** and **[2-pyz]_n** are stable toward air and moisture. However, this is no longer true for their CHCl₃ solutions, in which both compounds dissociate to a large extent (¹¹B NMR spectroscopic control;⁷ e.g., **1-pyz·1**: δ(¹¹B) = 50.1; cf. the free Lewis acid **1** [δ(¹¹B) = 70.5] and the more stable adduct **1-pic** [δ(¹¹B) = 0.4,⁶ pic = γ-picoline; Scheme 2]). The ¹¹B chemical shift observed for **1-pyz·1** is thus a weighted average between that of the pyrazine adduct and that of uncomplexed **1** bearing a three-coordinate boron center. Consequently, the ¹¹B NMR spectrum of **1-pyz·1** is dependent on temperature and on the concentration of the sample. Similar results are obtained when a mixture of **2** and pyz is investigated, and it may therefore be concluded that the existence of stable macromolecules **[2-pyz]_n** is restricted to the solid state.

(7) Nöth, H.; Wrackmeyer, B. Nuclear Magnetic Resonance Spectroscopy of Boron Compounds. In *NMR Basic Principles and Progress*; Diehl, P., Fluck, E., Kosfeld, R., Eds.; Springer-Verlag: Berlin, 1978.

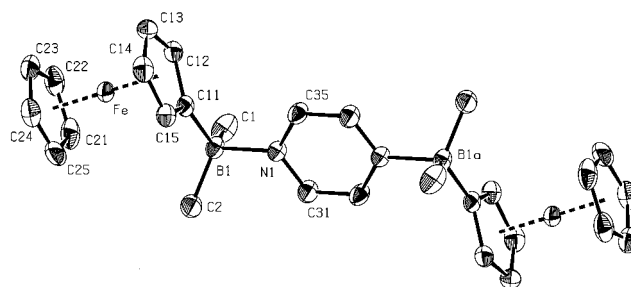


Figure 1. Molecular structure of **1-pyz·1**. Elements are represented by thermal ellipsoids at the 50% level. Selected bond lengths (Å), angles and torsion angles (deg): B(1)–N(1) 1.683(5), B(1)–C(11) 1.612(5), N(1)–C(31) 1.327(5), N(1)–C(35) 1.331(5), C(31)–C(35a) 1.378(5); N(1)–B(1)–C(1) 103.1(3), N(1)–B(1)–C(2) 105.3(3), N(1)–B(1)–C(11) 104.4(3), C(1)–B(1)–C(2) 114.3(3), C(1)–B(1)–C(11) 115.3(3), C(2)–B(1)–C(11) 112.8(3); C(12)–C(11)–B(1)–N(1) 102.4(4), C(11)–B(1)–N(1)–C(35) −21.9(4). Symmetry related atoms a: (−*x*, 1−*y*, −*z*).

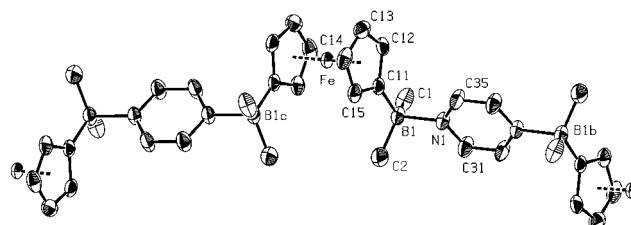


Figure 2. Molecular structure of **[2-pyz]_n** (toluene omitted for clarity). Elements are represented by thermal ellipsoids at the 50% level. Selected bond lengths (Å), angles and torsion angles (deg): B(1)–N(1) 1.711(3), B(1)–C(11) 1.603(4), N(1)–C(31) 1.337(4), N(1)–C(35) 1.342(4), C(31)–C(35b) 1.371(4); N(1)–B(1)–C(1) 103.7(2), N(1)–B(1)–C(2) 105.3(2), N(1)–B(1)–C(11) 104.4(2), C(1)–B(1)–C(2) 113.2(2), C(1)–B(1)–C(11) 113.9(2), C(2)–B(1)–C(11) 114.7(2), C(12)–C(11)–B(1)–N(1) 81.3(3), C(11)–B(1)–N(1)–C(35) −8.8(3). Symmetry related atoms: b (−*x*, 1−*y*, −*z*); c (1/2−*x*, *y*, 1/2−*z*).

Elemental analysis results were consistent with the proposed diadduct structure of **1-pyz·1** and with the aimed-for composition of **[2-pyz]_n**. This conclusion was confirmed by X-ray crystal structure analyses on **1-pyz·1** (Figure 1) and **[2-pyz]_n** (Figure 2).

The BMe₂·pyz substituents in **1-pyz·1**, as well as in **[2-pyz]_n**, are all rotated about the C(11)–B(1) axis such that both methyl groups point toward the iron core. The pyrazine ring, which almost bisects the C(1)–B(1)–C(2) angle, is placed in a plane perpendicular to the cyclopentadienyl ring. A similar structural motif has been observed in **1-bipy·1** (Scheme 2),⁶ as well as in the case of ferrocene-based tris(1-pyrazolyl)borate ligands.^{8–10} The crystal lattice of **[2-pyz]_n** consists of discrete stacks of pyrazine and ferrocene; the shortest intermolecular Fe–Fe distances are 5.710(1) Å.

The boron–nitrogen bond lengths of **1-pyz·1** (B(1)–N(1) = 1.683(5) Å) and **[2-pyz]_n** (B(1)–N(1) = 1.711(3) Å) are significantly longer than those of almost all other adducts between sp²-nitrogen donors and tetracoordinate boron atoms currently included in the Cambridge

(8) Jäkle, F.; Polborn, K.; Wagner, M. *Chem. Ber.* **1996**, *129*, 603.

(9) de Biani, F. F.; Jäkle, F.; Spiegler, M.; Wagner, M.; Zanella, P. *Inorg. Chem.* **1997**, *36*, 2103.

(10) Herdtweck, E.; Peters, F.; Scherer, W.; Wagner, M. *Polyhedron* **1998**, *17*, 1149.

Crystal Structure File (Release 2.3.7 UNIX 98/1).¹¹ This finding is consistent with the low basicity of pyrazine ($pK_a(1) = 0.65$, $pK_a(2) = -5.78$; in water, 27 °C).¹² The dinuclear adduct **1**·bipy·**1**, in which pyrazine is substituted for 4,4'-bipyridine, possesses B(1)–N(1) bond lengths of 1.682(5) and 1.689(4) Å (two crystallographically independent molecules in the asymmetric unit),⁶ which are very similar to those of **1**·pyz·**1**. In CHCl₃ solution, however, **1**·bipy·**1** dissociates to a far lesser extent than **1**·pyz·**1**, which can easily be explained by the higher basicity of 4,4'-bipyridine compared to pyrazine (4,4'-bipy: $pK_a(1) = 4.82$, $pK_a(2) = 3.17$; in water, 25 °C).⁶ Thus, the correlation between the strength of a dative B–N bond and the length of this bond in the solid state must not be overemphasized. The unusually long B–N bond in **1**·pyz·**1** and [**2**·pyz]_n is also reflected by a smaller degree of pyramidalization of the boron centers, which do not possess an ideal tetrahedral geometry [e.g., C(1)–B(1)–C(2) = 114.3(3)° (**1**·pyz·**1**), 113.2(2)° ([**2**·pyz]_n)]. However, unfavorable steric interactions between the methyl groups at boron and the bulky ferrocene moiety may also contribute to the flattening of the BMe₂ fragment.

Thermal analysis of [**2**·pyz]_n by DSC¹³ (heating rate 10 °C min^{−1}; inert gas N₂) revealed no changes of the material up to temperatures as high as 140 °C. Upon further heating, a sharp signal caused by an endothermic transition was observed [onset/peak temperatures: $T(\text{on}) = 144$ °C, $T(\text{peak}) = 149$ °C ($p = \text{const}$); $T(\text{on}) = 140$ °C, $T(\text{peak}) = 147$ °C ($V = \text{const}$)]. The fact that the event is independent of whether the thermal scans are run at constant pressure or at constant volume indicates the transition to be due to crystal melting. In contrast to its behavior in solution, [**2**·pyz]_n thus possesses a surprisingly high thermal stability in the solid state.

Pyrazine was chosen as the bridging element between the ferrocene building blocks, because its corresponding diquaternary salts [R·pyz·R]²⁺ (R = alkyl) are very strong electron acceptors.^{14,15} For example, the exceptionally stable 7 π electron radical [Et·pyz·Et]^{•+} (Scheme 2) is formed already at potential values as anodic as $E^\circ = +0.4$ V (vs SCE).¹⁴ When both alkyl groups of [R·pyz·R]²⁺ are substituted for boranes BR₃, the resulting neutral diadducts R₃B·pyz·BR₃ are still likely to preserve some of the electron-accepting potential of the parent dications. On the other hand, tetracoordination of the boron center(s) in **1** and **2** by 1 and 2 equiv of γ -picoline results in a pronounced cathodic shift of the Fe(II)/Fe(III) redox potential compared to the parent ferrocene ($E^\circ = +0.20$ V, **1**·pic; -0.01 V, **2**·(pic)₂; $+0.49$ V, (C₅H₅)₂Fe; DMF, vs SCE).⁶ One may thus anticipate charge-transfer interactions to occur between the electron-rich ferrocene fragments and the electron-poor pyrazine adduct bridges in **1**·pyz·**1** and [**2**·pyz]_n. In fact, the dark colors of both materials in the solid state (red-brown and green, respectively) are most easily explained

by this proposed electronic coupling. Due to the pronounced dissociation of **1**·pyz·**1** in CH₂Cl₂ and DMF, we have not been able to gain a decent cyclic voltammogram on this compound. Therefore, the reader is referred to the closely related, but much more stable, 4,4'-bipyridine diadduct **1**·bipy·**1**, which was found to give the expected electrochemical responses.⁶ A reversible two-electron ferrocene-centered oxidation ($E^\circ = +0.17$ V) is followed by two reversible one-electron bipy-centered reductions ($E^\circ = -1.20$ V, -1.75 V; DMF, vs SCE). Compared to the parent ferrocene, the Fe(II)/Fe(III) transition in **1**·bipy·**1** is shifted by 0.32 V toward a more cathodic value, while the two reduction waves appear at potentials that are each about 0.64 V less negative than in the corresponding free 4,4'-bipyridine. Similar to the pyrazine adducts, **1**·bipy·**1** possesses a very dark color, ranging from black (crystalline state) to purple (CHCl₃ solution).

Our findings show that stable low-dimensional solid materials with promising electrical and optical characteristics can be generated from readily available diborylated ferrocenes **2** and difunctional pyridine bases. We are currently trying to further increase the electronic coupling within the polymeric rods by employing even more strongly electron-accepting heterocycles than pyrazine (cf. tetrazine, quinoxaline).

Experimental Section

General Information. All the experimental manipulations involving the synthesis of the concerned starting materials were carried out under a dry and prepurified argon atmosphere, using Schlenk techniques rigorously excluding moisture and air. Solvents were freshly distilled under N₂ from Na/K alloy–benzophenone (hexane, toluene) or from CaH₂ (CH₂Cl₂, CHCl₃) prior to use. MS (FAB/CI mode): Finnigan MAT 90. IR: Perkin-Elmer 1650 FTIR. NMR: JEOL JMN-GX 400 and Bruker DPX 400. ¹¹B NMR spectra were referenced to external BF₃·Et₂O. Thermal analyses: Netzsch DSC 404 high-temperature furnace, thermocouple Pt/Rh, Perkin-Elmer TGA 7 thermobalance equipped with a Balzers QMG 420 mass spectrometer. Elemental analyses: Microanalytical Laboratory of the Technische Universität München.

Starting Materials. The ferrocene derivatives **1** and **2** were prepared using literature procedures.⁵

Preparation of **1·pyz·**1**:** At ambient temperature, a colorless solution of pyrazine (0.09 g, 1.12 mmol) in toluene (5 mL) was added dropwise to an orange-red solution of **1** (0.50 g, 2.21 mmol) in toluene (10 mL). The reaction mixture, which instantaneously adopted a dark red color, was stirred for 2 h. After that, the amount of solvent was slowly reduced in vacuo until a purple microcrystalline precipitate formed. The product was collected on a frit (G3), triturated with hexane (5 mL), and dried in vacuo. The filtrate was kept at -30 °C overnight to yield a second crop. Yield: 0.25 g (42%). Dark red-brown X-ray quality crystals were obtained from toluene/hexane (1:1) at -30 °C.

MS (CI): m/e 347 ($M^+ - \text{Fc}$; 9). IR (KBr, cm^{−1}): 1626(vw), 1479(w), 1418(s), 1112(m), 1098(s), 1083(s), 1060(s). ¹¹B NMR (128.3 MHz, CDCl₃): $\delta = 50.1$ ($h_{1/2} = 300$ Hz). ¹H NMR (400 MHz, CDCl₃): $\delta = 0.66$ (s, 12H, BCH₃), 4.05 (s, 10H, C₅H₅), 4.26, 4.47 (2 × 4H, C₅H₄), 8.62 (s, 4H, pyz). Anal. Calcd for C₂₈H₃₄B₂Fe₂N₂ (531.91): C, 63.23; H, 6.44; N, 5.27. Found: C, 63.10; H, 6.59; N, 5.09.

Preparation of [2**·pyz]_n.** A red solution of **2** (0.19 g, 0.71 mmol) in CH₂Cl₂ (15 mL) was layered in a Schlenk tube with neat toluene (15 mL) and then with a solution of pyrazine (0.06 g, 0.75 mmol) in toluene (10 mL). After 7 days, a homogeneous

(11) Allen, F. H.; Kennard, O.; Taylor, R. *Acc. Chem. Res.* **1983**, *16*, 146.

(12) Chia, A. S.; Trimble, R. F., Jr. *J. Phys. Chem.* **1961**, *65*, 863.

(13) Haines, P. J. *Thermal Methods of Analysis, Principles, Applications and Problems*; Blackie Academic Press: London, 1995.

(14) Kaim, W. *Rev. Chem. Intermed.* **1987**, *8*, 247.

(15) Kaim, W.; Schulz, A.; Hilgers, F.; Hausen, H.-D.; Moscherosch, M.; Lichtblau, A.; Jordanov, J.; Roth, E.; Zalis, S. *Res. Chem. Intermed.* **1993**, *19*, 603.

purple reaction mixture had formed, which was stored at 5 °C for several days to give dark green X-ray quality crystals of $[2\cdot\text{pyz}]_n$. Yield: 0.15 g (40%).

IR (KBr, cm^{-1}): 1653(vw), 1481(w), 1430(m), 1415(vs), 1108-(m), 1079(s), 1058(m). Anal. Calcd for $[\text{C}_{18}\text{H}_{24}\text{B}_2\text{FeN}_2]\cdot 2[\text{C}_7\text{H}_8]$ (530.15): C, 72.50; H, 7.61; N, 5.28. Found: C, 71.97; H, 7.55; N, 5.60.

X-ray Structure Determinations: $1\cdot\text{pyz}\cdot 1$. Data were collected on an air-stable dark red-brown needle ($0.94 \times 0.15 \times 0.15$ mm) at -110 ± 3 °C by using a NONIUS CAD4 diffractometer with graphite-monochromated Mo K α radiation ($\lambda = 0.71073$ Å) to $2\theta_{\text{max}}$ of 52.1° ; $[\text{C}_{28}\text{H}_{34}\text{B}_2\text{Fe}_2\text{N}_2]$, fw = 531.91, monoclinic, space group $P2_1/n$ (I.T. No.: 14), $a = 5.976(2)$ Å, $b = 16.620(2)$ Å, $c = 12.874(4)$ Å, $\beta = 91.08(2)^\circ$, $V = 1278.4(6)$ Å³ (based on 25 reflections; $44.4^\circ < 2\theta < 51.4^\circ$), $Z = 2$, $D_c = 1.382$ g cm^{-3} , $\mu(\text{Mo K}\alpha) = 11.5$ cm^{-1} (absorption correction not applied); 2846 data measured, 2507 unique, 2220 observed [$I > 2\sigma(I)$]. Non-hydrogen atoms were refined anisotropically, and hydrogen atoms were refined isotropically, 222 parameters refined, 11.3 data per parameter, residual electron density $+0.59$ e Å⁻³, -0.56 e Å⁻³, $R1 = 0.0555$ [all data], $wR2 = 0.1290$ [all data], minimized function was $\sum w(F_o^2 - F_c^2)^2$. The final fractional atomic coordinates are given in the Supporting Information.

$[2\cdot\text{pyz}]_n$. Data were collected on an air-stable dark green platelet ($0.50 \times 0.30 \times 0.13$ mm) at 20 ± 1 °C by using an image plate diffraction system (IPDS, STOE) with graphite-monochromated Mo K α radiation ($\lambda = 0.71073$ Å); the compound crystallizes together with 2 equiv of toluene, which is not disordered, $[\text{C}_{18}\text{H}_{24}\text{B}_2\text{FeN}_2]\cdot 2[\text{C}_7\text{H}_8]$, fw = 345.87 (+184.28), monoclinic, space group $A2/n$ (I.T. No.: 15), $a = 8.0084(5)$ Å, $b = 16.7786(14)$ Å, $c = 21.9368(10)$ Å, $\beta = 100.298(6)^\circ$, $V = 2900.2(3)$ Å³, $Z = 4$, $D_c = 1.214$ g cm^{-3} , $\mu(\text{Mo K}\alpha) = 5.4$ cm^{-1} (absorption correction not applied); 9460 data measured, 1264 unique, 1060 observed [$I > 2\sigma(I)$]. All of the crystals investigated turned out to be partial merohedric twins. Using the software tool TWIN,¹⁶ we were able to integrate the data of the nontwinned parts. We obtained two half-records which we used to solve and refine the structure. Non-hydrogen atoms

were refined anisotropically, and hydrogen atoms were calculated in ideal positions (riding model), 168 parameters refined, 7.5 data per parameter, residual electron density $+0.15$ e Å⁻³, -0.15 e Å⁻³, $R1 = 0.0383$ [all data], $wR2 = 0.0731$ [all data], minimized function was $\sum w(F_o^2 - F_c^2)^2$. The final fractional atomic coordinates are given in the Supporting Information.

Neutral atom scattering factors for all atoms and anomalous dispersion corrections for the non-hydrogen atoms were taken from the *International Tables for X-ray Crystallography*.¹⁷ The structures were solved by direct methods. All calculations were performed on a DEC 3000 AXP workstation with the STRUX-V system,¹⁸ including the programs PLATON-92,¹⁹ PLUTON-92,¹⁹ SHELXS-86,²⁰ SIR-92,²¹ and SHELXL-93.²²

Acknowledgment. This work was supported by the Deutsche Forschungsgemeinschaft and the Fonds der Chemischen Industrie.

Supporting Information Available: X-ray structural data for $1\cdot\text{pyz}\cdot 1$ and $[2\cdot\text{pyz}]_n$, including a summary of crystallographic parameters, atomic coordinates, bond lengths and angles, and thermal parameters. This material is available free of charge via the Internet at <http://pubs.acs.org>. The data have also been deposited at the Cambridge Crystallographic Data Centre (CCDC). Any request to the CCDC for this material should quote the full literature citation and the reference numbers 119540 ($1\cdot\text{pyz}\cdot 1$) and 119541 ($[2\cdot\text{pyz}]_n$).

OM990594I

(17) *International Tables for Crystallography*; Wilson, A. J. C., Ed.; Kluwer Academic Publishers: Dordrecht, Netherlands, 1992; Vol. C, Tables 6.1.1.4 (pp 500–502), 4.2.6.8 (pp 219–222), and 4.2.4.2 (pp 193–199).

(18) Artus, G.; Scherer, W.; Priermeier, T.; Herdtweck, E. *STRUX-V, A Program System to Handle X-ray Data*; TU München: Germany, 1994.

(19) Spek, A. L. *Acta Crystallogr. A* **1990**, *46*, C34.

(20) Sheldrick, G. M. *SHELXS-86: Program for Crystal Structure Solutions*; Universität Göttingen: Germany, 1986.

(21) Altomare, A.; Cascarano, G.; Giacovazzo, C.; Guagliardi, A.; Burla, M. C.; Polidori, G.; Camalli, M. *SIR-92*; University of Bari: Italy, 1992.

(22) Sheldrick, G. M. *SHELXL-93. In Crystallographic Computing 3*; Sheldrick, G. M., Krüger, C., Goddard, R., Eds.; Oxford University Press: Oxford, 1993.

(16) TWIN; IPDS Operating System Version 2.6; STOE & CIE GmbH: Darmstadt, Germany, 1995.